Diffusion-Thermo Effects on Heat Transfer from a Cylinder in Cross Flow

O. E. TEWFIK*
Corning Glass Works, Corning, N. Y.
E. R. G. ECKERT†
University of Minnesota, Minneapolis, Minn.
AND
L. S. JUREWICZ‡
National Research Council, Ottawa, Canada

Measurements are described of the distributions of the heat transfer coefficient and adiabatic wall temperature around a 3-in.-o.d. circular cylinder with a stainless steel woven wire porous wall, and with its axis normal to a low-speed air stream. Helium was injected through the cylinder wall into the boundary layer at an approximately uniform rate per unit area of outside cylinder surface in the range of 5.45 to 25.8 lbm/hr-ft². The range of freestream velocity was 62.9 to 99.0 fps and of freestream Reynolds number based on cylinder diameter 1.01 $\times 10^5$ to 1.59 $\times 10^5$. It was determined that, when the heat exchange between cylinder and air stream was zero, the wall temperature exceeded the freestream temperature by up to 86°F, depending upon location on cylinder circumference, helium injection rate, freestream velocity, and properties. This phenomenon is due to the diffusion-thermo effect. The measured heat transfer coefficients at the forward stagnation point agreed fairly well with analyses that did not include the diffusion-thermo effect provided that the heat transfer coefficient was defined with the difference between the wall temperature and the adiabatic wall temperature.

Nomenclature

b = thickness of stainless steel shell of model = 0.035 in.
c_p = specific heat of helium at constant pressure
d = outside diameter of model = 3 in.
h = convective heat transfer coefficient, defined by Eq. (4)
k = thermal conductivity
k_s = thermal conductivity of stainless steel shell of model
$\dot{m}$ = local mass injection rate of helium per unit area of outside cylinder surface
$\bar{\dot{m}}$ = average mass injection rate of helium per unit area of outside cylinder surface
p = pressure
q_c = heat flux by circumferential conduction in stainless steel shell, Eq. (3)
q_r = radiative heat flux from model surface to tunnel walls, Eq. (2)
q_w = heat flux between model and air stream, defined by Eq. (1)
r = outside cylinder radius
T = temperature
T_a = adiabatic wall temperature at which $q_w = 0$
T_c = temperature of helium inside model
T_t = temperature of inside surface of tunnel test section
T_w = temperature of outside surface of model
u = velocity component in the boundary layer along x direction
v = radial velocity component
x = space coordinate along the circumference of the cylinder, measured from forward stagnation point
β = velocity gradient at the forward stagnation point = du_e/dx
ϵ = emissivity of model surface
ν = kinematic viscosity
θ = angle between a cylinder radius and the radius through the forward stagnation point
ρ = density
σ = Stefan-Boltzmann constant
f_d = $\dot{m}(Re_d)^{1/2}/\rho_\infty u_\infty$
f_w = $\dot{m}\,(Re_x)^{1/2}/\rho_e u_e = f_d(u_\infty/\beta d)^{1/2}$
Nu_d = hd/k_∞
Re_d = du_∞/ν_∞
Re_x = xu_e/ν_e

Subscripts

e = outer edge of boundary layer
w = model wall
∞ = freestream

Introduction

THE process of injecting a gas through a porous wall in order to modify the characteristics of the adjacent boundary layer has received considerable attention in the past decade. In particular, the forced convection heat transfer to the wall can be reduced considerably, and the process is therefore referred to as mass transfer cooling.

When gases different from the mainstream are injected, the boundary layer becomes a binary system, and pertinent analyses have been reviewed recently.[1] However, thermal diffusion was not considered in these calculations. Because of this phenomenon, lighter species tend to migrate towards warmer regions in multicomponent systems. In a similar manner, concentration gradients will give rise to a transport of energy on a molecular level, i.e., to a transport of heat in addition to the familiar heat conduction as described by Fourier's law. This is referred to as the diffusion-thermo effect.[2] This energy contribution has been neglected, to date, in engineering applications of heat transfer on the a priori assumption that it is second order in comparison with the Fourier heat conduction. A recent analysis and comparison with previous measurements,[3] however, demonstrated for the first time appreciable effects on heat transfer and adiabatic wall temperature which occur when helium is

Received by IAS September 29, 1962; revision received April 23, 1963. Communication from the Heat Transfer Laboratory, University of Minnesota, Minneapolis, Minn. This research was supported by the U. S. Air Force through the Air Force Office of Scientific Research of the Air Research and Development Command under Contract No. AF 49 (638)-558. The help of Ji-Wu Yang in taking part of the data is acknowledged gratefully.

* Project Engineer. Member AIAA.
† Professor of Mechanical Engineering and Director of the Heat Transfer Laboratory. Member AIAA.
‡ Assistant Research Officer.

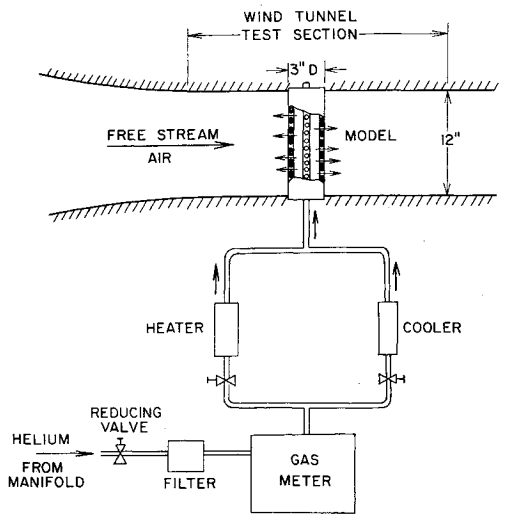

Fig. 1 Schematic sketch of apparatus

injected into a laminar boundary layer. Subsequent measurements demonstrated the same for the first time in turbulent boundary layers.[4] From additional measurements,[5] the heat flux due to the diffusion-thermo effect actually was determined in a special case to exceed even the familiar Fourier heat flux.

With such evidence of the importance of this effect in multicomponent systems, it was decided to continue efforts in its study by measuring the distribution of heat transfer around a cylinder in cross flow with helium injection. The measurements and their results are described below, and the results at the forward stagnation point are compared with the predictions of available analyses which do not include the diffusion-thermo effect.[6-8]

Apparatus

A schematic diagram of the entire apparatus is shown in Fig. 1. A 3-in.-o.d. circular cylinder was mounted with its axis normal to the air stream in the test section of a low-speed wind tunnel. Helium flowed into the cylinder and escaped through the porous walls into the adjacent boundary layer. The more important components of the apparatus are described below in some detail.

Model and Instrumentation

The model, shown in detail in Fig. 2, already has been used in a previous investigation with air injection.[9] It consists of a 3-in.-o.d. circular porous wall cylinder 1 ft in length. The porous wall is fabricated from two stainless steel woven wire screens of mesh counts 50 × 250 and 12 × 64 wires/in. With one on top of the other, the screens were sintered and calendered to an average thickness of 0.035 in. The surface of the porous shell is not quite smooth, but contains more or less regular depressions approximately 0.005 in. in depth. The stainless steel porous shell is lined with Fiberglas filter paper to a thickness of about 0.5 in.

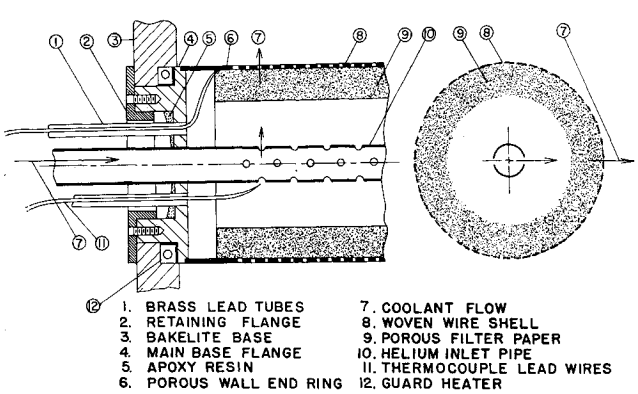

Fig. 2 Sectional views of model

Thermocouple junctions of 36-gage iron-constantan wire were welded to the inside of the porous shell around the periphery of the cylinder at its middle plane, and at 3 in. on either side of the middle plane. After installation, the thermocouples were calibrated by immersing the model in an oil bath, with temperature control. These thermocouples are assumed to measure the temperature of the outside surface of the model, since the temperature difference across the thin porous shell was negligible.

Helium flowed into the model through a 0.5-in.-o.d. steel tube, coaxial with the model, and escaped through a series of small holes into the inside of the model. At this point, its temperature was measured by a series of 36-gage iron-constantan thermocouples fastened along the steel tube. More details regarding the model and instrumentation may be found in Ref. 9.

Wind Tunnel

The model was mounted with its axis vertical and normal to the air stream in the 1- × 2-ft test section of the wind tunnel of the Heat Transfer Laboratory. The tunnel operated continuously in an open circuit with air inlet and outlet located outdoors. The air speed was changed in steps from about 60 to 150 fps. The tunnel has a low turbulence level of approximately 0.2%.

Helium Flow System

Helium flowed from a bank of 20 bottles into a manifold and then through a reducing valve to reduce its pressure to about 100 psig. It then passed through an American Iron case gas meter, type 80C, where its volume flow rate was measured. By measuring the temperature and pressure at inlet and outlet of the meter, respectively, the helium density was determined and hence its mass flow rate. After the meter, the helium passed through a variable input electric heater and/or a cooler consisting of a coil immersed in a cold bath of dry ice in ethyl alcohol. In this way the helium temperature was controlled. Finally the helium was discharged into the inside of the model and escaped through its porous walls into the adjacent boundary layer.

Method of Determining Local Convective Heat Flux

The local heat flux q_w exchanged between model surface and boundary layer was determined by applying the first law

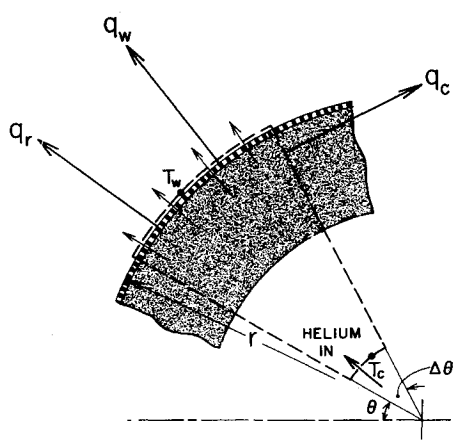

Fig. 3 Control volume for energy balance to determine local heat flux

of thermodynamics to the open system indicated in Fig. 3. The system extends a length L normal to the paper and contains a segment of the model subtending a small angle $\Delta\theta$ at the model axis.

The following expression for the local convective heat flux results:

$$q_w = \dot{m}c_p(T_c - T_w) - q_r - q_c \quad (1)$$

where

$$q_r = \epsilon\sigma(T_w^4 - T_t^4) \quad (2)$$

$$q_c = -k_s b(d^2T/d\theta^2)/r^2 \quad (3)$$

In the just-mentioned derivation, it is assumed that the temperature of the helium as it leaves the stainless steel shell is identical with T_w, the temperature of the outside surface of the shell. This assumption has been ascertained by previous measurements with air.[10] It also is assumed that the circumferential heat conduction through the filter paper is negligible compared to that in the steel shell. This is justifiable since the porosity of filter paper is quite high, about 90%, and hence its thermal conductivity approaches that of helium. The emissivity ϵ of the stainless steel shell was measured to be 0.27. By measuring $\dot{m}$, T_c, T_w, T_t, the heat flux q_w could be calculated with Eq. (1).

With the existence of helium (which is much lighter than air) in the boundary layer, some free convection effects on heat transfer may be expected. Such effects were estimated and were shown to be negligible.[11] Also, axial heat conduction was investigated and shown tc be negligible in the measurements reported here.[11]

Experimental Procedure

The location of the forward stagnation point was determined by injecting heated air through the model walls and observing the readings of a particular wall thermocouple while rotating the model. When the thermocouple was exactly at the forward stagnation point, its reading would be a minimum in comparison with neighboring positions. This procedure was repeated for the two adjacent thermocouples, and, from the average of the location of all three minimum values, the location of the forward stagnation point finally was determined.[11]

The helium mass flow rate through the gas meter was set at a particular value. By adjusting the relative flow through the heater and cooler, and the electric input to the heater, the helium temperature inside the model was adjusted to the desired level. After establishing steady state, the output of all the wall thermocouples was read along with that of the thermocouples inside the model, a shielded thermocouple in the tunnel freestream to indicate T_∞ and a thermocouple taped to the interior wall of the tunnel test section to indicate T_t. During the course of these measurements, a check of the wall temperature at the forward stagnation point and the helium temperature inside the model showed that neither varied by more than $\pm$ 0.1°F, and hence steady state was considered to be established satisfactorily.

Keeping the helium mass flow rate through the model unchanged, T_c was adjusted to various levels, and the procedure in the preceding paragraph was repeated. In this way, data were taken to determine the local heat flux at a given mass injection rate, but at various levels of T_w. Reproducibility of the data was checked randomly, and agreement was obtained in all cases within less than 5%, usually within 2 or 3%.

The procedures just described were repeated for other values of helium injection rates, as indicated in Table 1.

During any run, the pressure of helium inside the model was of course uniform, but the pressure distribution outside the model was not. In particular, the outside pressure was a maximum at the forward stagnation point, and hence the pressure difference across the filter paper and stainless steel shell was a minimum there. Consequently, the local helium injection rate deviated slightly from uniformity around the model. To determine accurately the local mass injection rate, the pressure distribution with air injection was measured as described in the Appendix. From this, the distribution of mass injection around the cylinder was determined.[9]

Table 1 Injection rates and freestream conditions

Case	u_∞, fps	T_∞, °F	$Re_d \times 10^{-5}$	$\bar{m}$, lbm/hr-ft²
1	85.0 ± 2%	59.2 ± 6	1.31 ± 2%	5.45 ± 3%
2	85.8 ± 2%	61.4 ± 5	1.34 ± 2%	15.7 ± 1.5%
3	83.9 ± 2%	63.7 ± 16	1.27 ± 4%	25.8 ± 2%
4	62.9 ± 2%	47.2 ± 3	1.01 ± 2%	9.99 ± 0.3%
5	85.9 ± 2%	58.2 ± 3	1.33 ± 2%	10.1 ± 0.8%
6	99.0 ± 2%	47.2 ± 2	1.59 ± 2%	10.0 ± 0.5%

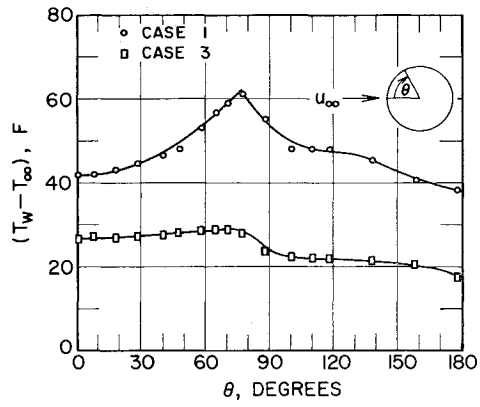

Fig. 4 Temperature distribution around cylinder

Results and Discussion

Heat transfer measurements were obtained at each of three values of average rates of helium injection denoted as cases 1–3 in Table 1, at approximately the same tunnel air speed and temperature. Also, at an average injection rate of 10.0 lbm/hr-ft², measurements were taken at each of three different values of tunnel air speed. These are listed as cases 4–6 in Table 1. The latter procedure was necessary to investigate separately the effects of changing freestream velocity on heat transfer and other results. For each of the cases indicated in Table 1, test runs were made at four or five different wall temperature levels, as explained in detail in the preceding section. The average injection rate changed slightly from run to run, and so did the freestream velocity and temperature. Hence, all values shown in Table 1 are average quantities for the runs constituting the particular case under consideration. Beside each number, the maximum deviations from the average are indicated.

The wall temperature distribution around the cylinder with helium injection is presented in Fig. 4 for the smallest and highest injection rates. Similar distributions occurred for the intermediate injection rates.

Heat Transfer at the Forward Stagnation Point

Using Eqs. (1–3), the convective heat flux q_w at the forward stagnation point was computed at a given helium injection rate for several levels of T_w. The results were plotted in Fig. 5a for cases 1–3 and in Fig. 5b for cases 4–6. (Refer to Table 1 for the definitions of the various cases.) In all cases, q_r was not more than 2% of q_w. The conduction correction q_c in Eq. (1) turned out to be a few Btu/hr-ft² at the most and hence was neglected altogether, due to the uncertainty in

determining the second derivative of temperature with respect to θ. By inspecting Figs. 5a and 5b, two conclusions may be drawn regarding the dependence of q_w on $(T_w - T_\infty)$: 1) the heat flux is a linear function of the temperature difference as in other cases of forced convection heat transfer; and 2) in contrast with other cases of forced convection heat transfer in low-speed flow, the heat flux does not vanish when the temperature difference between wall and freestream vanishes. In the present measurements, the heat flux vanishes when the wall temperature is higher than the freestream temperature by up to 46°F, depending on the helium injection rate and the freestream velocity. The wall temperature under this condition of vanishing heat flux will be termed the "adiabatic wall temperature," T_a. At adiabatic conditions, the wall is losing heat by the usual Fourier conduction but is gaining an equal amount by the diffusion-thermo effect, and hence the net heat transfer will be zero.[3] Adiabatic wall temperatures in low-speed flow, considerably different from freestream temperature, first were measured in turbulent boundary-layer flow with helium injection.[4] Later, the Fourier conduction heat flux and the diffusion-thermo heat flux were determined from the results of measurements.[5]

In the situation just discussed, it is necessary to define a heat transfer coefficient by the equation

$$q_w = h(T_w - T_a) \tag{4}$$

The conventional definition in low-speed flow in which T_∞ replaces T_a in Eq. (4) would lead to values for h between 0 and $\pm\infty$. The value of h as defined by Eq. (4) is the slope of the straight lines in Figs. 5a and 5b and is thus independent of $(T_w - T_a)$, at least within a moderate temperature range around the freestream temperature such as in the measurements reported here. From the two figures, h is seen to decrease as the helium injection rate is increased and as the freestream velocity is decreased. The adiabatic wall temperature, however, follows an opposite trend.

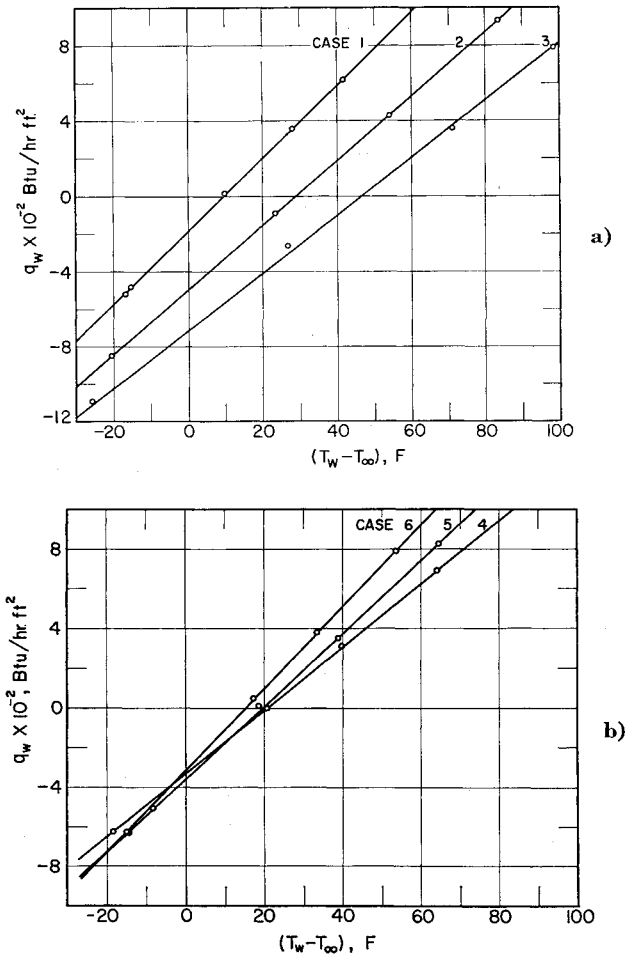

Fig. 5 Heat flux at forward stagnation point

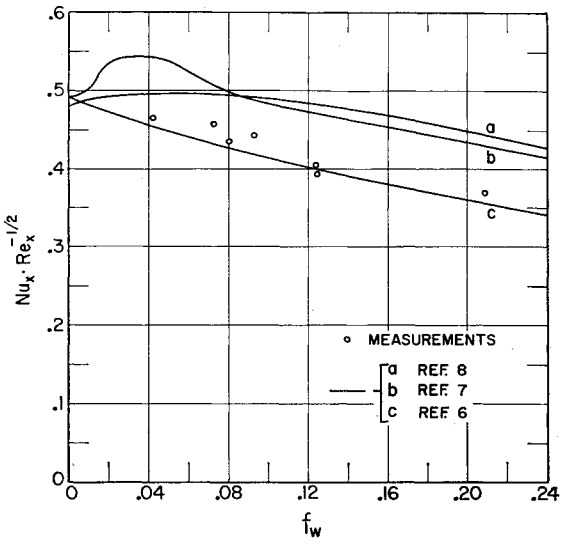

Fig. 6 Heat transfer at forward stagnation point—comparison with theory

In looking for theoretical predictions to compare with the results of measurements reported here, no analysis of heat transfer at the forward stagnation point including diffusion-thermo effects could be found. However, a calculation for laminar Couette flow[4] indicated that thermo-diffusion appears to have negligible effects on the heat transfer coefficient, provided that h is defined according to Eq. (4). On the assumption that this is also true at the forward stagnation point, the present experimental results can be compared with theoretical analyses in which thermo-diffusion was neglected. Among analytical solutions published in the literature, there are three that consider two-dimensional stagnation flow with helium injection into an air stream and with boundary conditions close to the one in the present experiments.

An analysis by Baron and Scott[6] considers freestream conditions of 570°R and 1 psia, and a ratio of the wall temperature to the freestream temperature equal to 1.25. The properties in the dimensionless parameters Nu, Re, and f_w are introduced for conditions at the edge of the boundary layer. An analysis by Hurley[7] solves the conservation equations on an analog computer with a temperature of 540°R at the outer edge of the boundary layer. The properties within the boundary layer were assumed independent of temperature. Properties introduced into the dimensionless parameters Nu, Re, and f_w were those at the outer edge of the boundary layer.

An analysis performed at the Heat Transfer Laboratory[8] considered a variety of boundary conditions. One set of calculations assumed a freestream temperature of 540°R and a ratio of wall to stream temperature equal to 1.2. In the present measurements, the stream temperature varied between 505° and 540°R, and the ratio of wall temperature to freestream temperature between 0.95 and 1.2. The experimentally determined heat transfer coefficients therefore can be compared readily with the results of the just-mentioned analyses. In calculating the groups Nu, Re, and f_w from the present measurements, the properties introduced were those of air at the respective mean free temperature of the test runs used in the calculation of the heat transfer coefficient.

The comparison between the three analyses and the experimental results is presented in Fig. 6. For a more detailed discussion of the analytical results, the reader is referred to Ref. 8. It may only be mentioned that the differences between the results of the three analyses are mainly due to the values of the thermal conductivity on which the

calculations were based. The agreement between the experimental results and the analytical values is quite satisfactory. This supports the conclusion reached in Refs. 3 and 4, that thermo-diffusion has a small effect on the heat transfer coefficient when it is defined by Eq. (4).

Next, the measured adiabatic wall temperature is compared with the results of Ref. 3, which is the only available analysis so far that includes thermo-diffusion effects on adiabatic wall temperature for rotationally symmetric stagnation point flow. In Fig. 13 of Ref. 3, the results of an "exact solution" are expressed in terms of the recovery temperature calculated with thermo-diffusion being neglected. This latter temperature is equal to the freestream temperature under the conditions of the present measurements. Figure 7 compares the experimental results with this analysis. The difference of approximately 10% may be due to the fact that the measurements deal with plane stagnation flow. The measured adiabatic wall temperatures in Fig. 7 are correlated closely by the empirical formula:

$$(T_a - T_\infty)/T_\infty = 0.43\, f_w \qquad (5)$$

Heat Transfer Distribution

The heat transfer coefficient at various angular locations around the cylinder was determined by methods similar to those described for the stagnation point. For cases 1–3, Re_d was approximately constant, but the injection rate was different. For these cases, the heat transfer coefficient expressed in dimensionless form as $Nu_d\, Re_d^{-1/2}$ is presented as function of θ in Fig. 8a and compared with the case of no injection in subcritical flow.[12]

From Fig. 8a it is evident that, at a particular location, the heat transfer coefficient is reduced as the helium injection rate is increased. At a given injection rate, however, the percentage reduction in the heat transfer coefficient is a maximum at the forward stagnation point, and decreases to a minimum around $\theta = 80°$. At the rear stagnation point, the reduction in the heat transfer coefficient due to injection is markedly less than at the forward stagnation point.

The shape of the heat transfer distribution on the solid cylinder is similar to the measured distributions with helium injection for cases 2 and 3 and shows the same main features. In particular, laminar separation of the boundary layer takes place approximately at $\theta = 80°$. An exception to this observation is case 1, which corresponds to the smallest injection rate and yet exhibits a behavior characteristic for transition in the boundary layer followed by turbulent separation. These two latter characteristics are typical of supercritical flow. The anomaly that supercritical flow occurred in case 1 but not in case 2 or 3, even though Re_d is about the same in all three cases and the injection rate is least for case 1, cannot be explained at present.

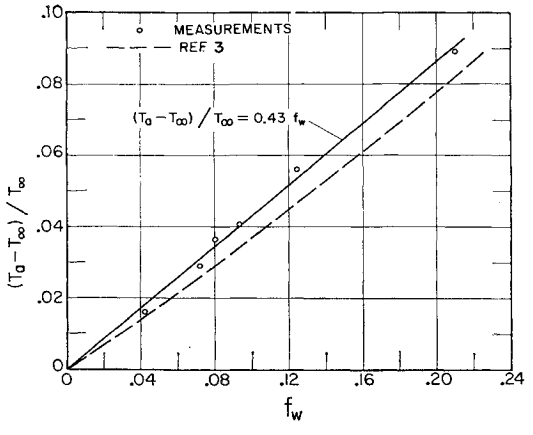

Fig. 7 Adiabatic wall temperature at forward stagnation point—correlation of results and comparison with theory

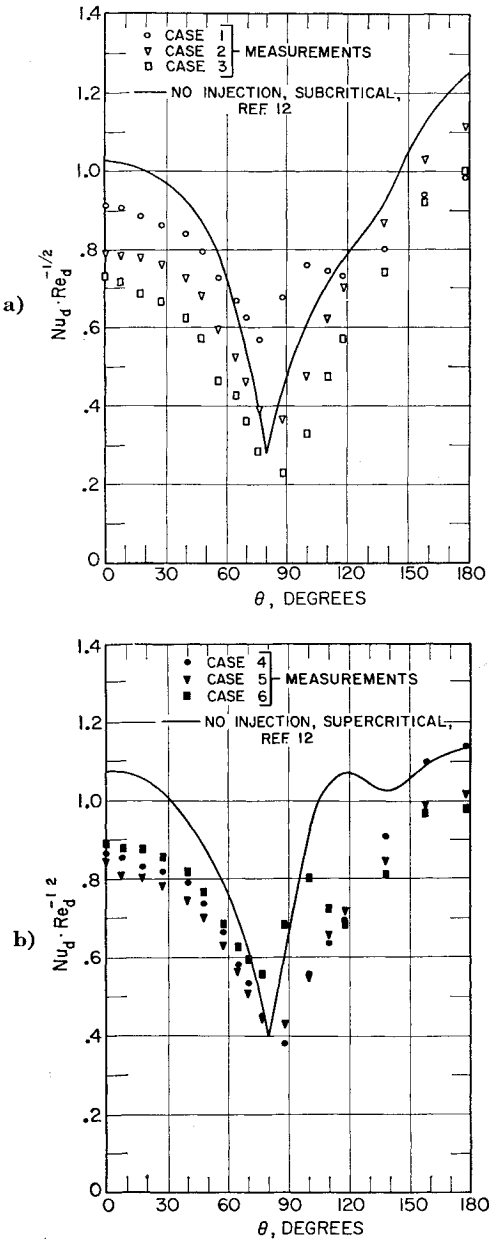

Fig. 8 Distribution of heat transfer coefficient

Presentation of the distribution of the heat transfer coefficient around the cylinder is continued in Fig. 8b for cases 4–6. In these cases, the injection rate was kept the same, but Re_d had values in the range of 1.01×10^5 to 1.59×10^5. The flow appears to be subcritical for cases 4 and 5 but clearly changes to supercritical for case 6, due to the increase in Re_d for the latter case. The distributions are again compared with the case of no injection for supercritical flow.[12] Unfortunately, the range of Re_d is too small and the scatter in the data is too large to make definite conclusions regarding the dependence of $Nu_d\, Re_d^{-1/2}$ on Re_d.

Adiabatic Wall Temperature Distribution

From figures similar to Figs. 5a and 5b, but constructed for other circumferential locations around the cylinder, the excess of adiabatic wall temperature over freestream temperature was determined, and the results are presented in Fig. 9a for the highest and smallest injection rates. It is seen that, although there is no heat exchange between cylinder and boundary layer, the cylinder walls are hotter than the freestream by up to 86°F, depending upon the injection rate and the circumferential location.

In dimensionless form, the distribution is presented for cases 1–3 in Fig. 9b. At a given injection rate, T_a is highest near the laminar separation point. At a given location, T_a increases as the injection rate increases. Figure 9c presents the distribution of T_a for cases 4–6. For case 6, transition

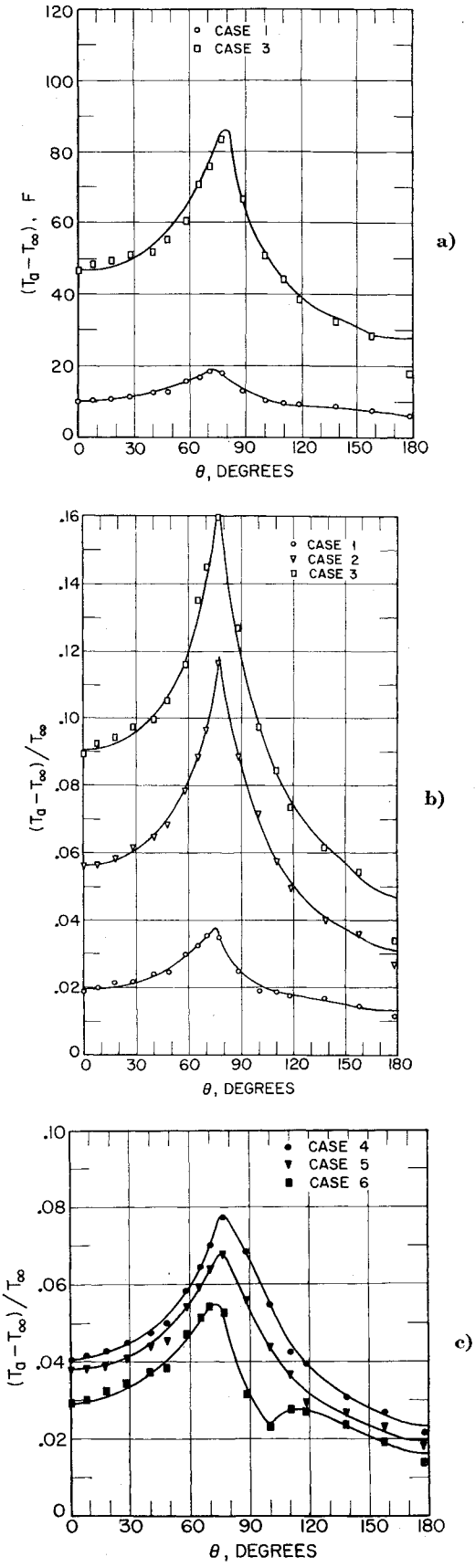

Fig. 9 Distribution of adiabatic wall temperature

to turbulence is clearly evident in agreement with a similar observation based upon the distribution of the heat transfer coefficient in Fig. 8b. In contrast to this clear indication of transition in Fig. 9c for case 6, no such evidence can be seen in Fig. 9b for case 1, for which the distribution of heat transfer coefficient indicated the possibility of transition. It may be that the transition in case 1, if any, was not sharp, or that T_a is not as sensitive to transition as the heat transfer coefficient. From Fig. 9c, it can be seen that T_a increases as the freestream velocity decreases, provided that the injection rate remains unchanged.

Summary and Conclusions

The distribution of heat transfer around a porous wall 3-in.-o.d. circular cylinder, with its axis normal to a low-speed air stream, was measured at various rates of helium injection, various levels of wall temperature, and various values of the freestream velocity. Analysis of the results showed that, when the heat exchange between the cylinder and the boundary layer was zero, the wall temperature—in this case termed the adiabatic wall temperature—exceeded the freestream temperature by up to about 86°F, depending upon the particular location around the cylinder, the helium mass injection rate, and the freestream velocity. This unusual phenomenon in low-speed flow is caused by the diffusion-thermo effect in the binary boundary layer.

At the forward stagnation point, the measured adiabatic wall temperature agreed within 10% with an analysis for rotationally symmetric stagnation point flow which takes thermo-diffusion into consideration.[3] The measured heat transfer coefficient agrees fairly well with analyses neglecting thermo-diffusion.[6–8] It appears that thermo-diffusion has no effect on the heat transfer coefficient provided it is defined, as in Eq. (4), in terms of the adiabatic wall temperature. A similar conclusion was obtained from an analysis of heat transfer in laminar Couette flow with helium injection.[4]

The distributions of the heat transfer coefficient and of the adiabatic wall temperature around the cylinder were determined. Both showed evidence of supercritical flow when $Re_d = 1.59 \times 10^5$ and subcritical flow when Re_d was about 1.3×10^5 or less except for case 1, in which the heat transfer coefficient showed some evidence of transition although the adiabatic wall temperature did not. The distribution of the heat transfer coefficient with helium injection had the same general shape as the corresponding distribution without injection. The main difference is that the former is generally smaller than the latter, with the deviation increasing as the injection rate increases. The percentage reduction in the heat transfer coefficient due to injection is a maximum at the forward stagnation point, and decreases to a minimum at the separation or transition point. The trends of variation of the adiabatic wall temperature with location, injection rate, or freestream velocity were opposite to those of the heat transfer coefficient.

Appendix: Measurements of Pressure Distribution

It is necessary to determine the velocity gradient at the forward stagnation point in order to correlate the heat transfer measurements and to compare them with theory. It is also interesting to investigate the effects of injection on the potential flow around the cylinder. For these two purposes, the pressure distribution with injection was measured and compared with that around a solid wall 3-in.-o.d. cylinder mounted in the same wind tunnel.[9]

Surface Pressure Probe

Since no provisions for pressure measurements were provided on the porous wall model, a special surface probe was

designed and constructed. It was fabricated out of steel tubing flattened to outside dimensions of 0.007 × 0.078 in. In operation, one probe side pressed against the porous wall of the cylinder, and a 0.018-in.-diam hole in the opposite probe side sensed the static pressure near the cylinder surface. The tip of the probe was sealed with silicone grease to make sure that the probe did not sense any dynamic pressure of the flow near the cylinder surface. The probe was fixed rigidly to the model with spring steel clips, with its tip in the horizontal central plane of the model. Reference 11 may be consulted for more details regarding the probe or measurements.

During the measurements, the probe response time was of the order of 3 to 5 min and hence was too large for using helium for injection purposes. Instead, air was injected at a rate of 0.0233 lbm/sec-ft^2, and pressure distribution measurements were taken at values of Re_d of 1.11×10^5 and 1.46×10^5. In addition, the surface probe was used to measure the pressure distribution around the solid wall model for $Re_d = 1.1 \times 10^5$, and the results were compared with previous measurements[9] using pressure taps.

Results

The pressure distributions are shown in Fig. 10. In comparing the results with the surface probe and the earlier results[9] using pressure taps on the same solid wall model, it is found that they are almost identical except in the region near the laminar separation point and downstream from it where discrepancies up to 20% exist.

A comparison of the results of air injection with those without injection, using the surface probe in both cases, reveals close agreement on the forward part of the cylinder. Discrepancies up to about 10%, however, exist near the laminar separation point and downstream from it. Apparently the injection process shifts the pressure distribution somewhat in the direction of supercritical flow. From the pressure distribution with air injection, the velocity gradient at the forward stagnation point was determined to be about 5% less than that in flow of an inviscid fluid.

It thus may be concluded that the injection process does not materially influence the pressure distribution on the front of the model or the velocity gradient at the forward stagnation point in particular. Near the laminar separation point and after, in the wake region, some influence may exist.

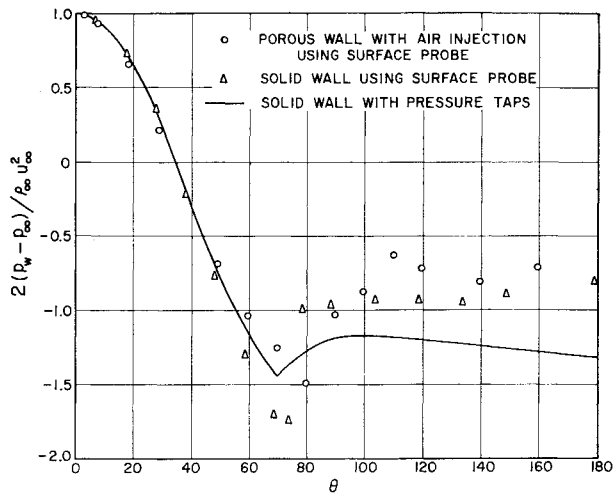

Fig. 10 Model pressure distribution

References

[1] Gross, J. F., Hartnett, J. P., Masson, D. J., and Gazley, C. J., "A review of binary laminar boundary layer characteristics," Intern. J. Heat Mass Transfer **3**, 198–221 (1961).

[2] Chapman, S. and Cowling, T. G., *The Mathematical Theory of Non-uniform Gases* (Cambridge University Press, Cambridge, England, 1952), 2nd ed., pp. 404–408.

[3] Baron, J. R., "Thermodynamic coupling in boundary layers," ARS J. **32**, 1053–1059 (1962).

[4] Tewfik, O. E., Eckert, E. R. G., and Shirtliffe, C. J., "Thermal diffusion effects on energy transfer in a turbulent boundary layer with helium injection," *Proceedings of the 1962 Heat Transfer and Fluid Mechanics Institute* (Stanford University Press, Stanford, Calif., 1962), pp. 42–61.

[5] Tewfik, O. E. and Shirtliffe, C. J., "On the coupling between heat and mass transfer," J. Aerospace Sci. **29**, 1009–1010 (1962).

[6] Baron, J. R. and Scott, P. B., "The laminar diffusion boundary layer with external flow field pressure gradients," Mass. Inst. Tech., Naval Supersonic Lab., TR 419 (1958).

[7] Hurley, D. G., "Mass transfer cooling in a boundary layer," Aeronaut. Quart. **XII**, Part 2, 165–188 (1961).

[8] Eckert, E. R. G., Minkowycz, W. J., Sparrow, E. M., and Ibele, W. E., "Heat transfer and friction in two-dimensional stagnation flow of air with helium injection," Intern. J. Heat Mass Transfer **6**, 245–248 (1963).

[9] Johnson, B. V., "Heat transfer from a cylinder in crossflow with transpiration cooling," M.S. Thesis, Univ. Minn. (1960).

[10] Tewfik, O. E., Eckert, E. R. G., and Jurewicz, L. S., "Measurement of heat transfer from a circular cylinder to an axial air stream with air injection into a turbulent boundary layer," Air Force Office Sci. Res. Rept. 1397 (1961).

[11] Jurewicz, L. S., "Transpiration cooling of a cylinder in cross flow with helium injection," M.S. Thesis, Univ. Minn. (1961).

[12] Schmidt, E. and Wenner, K., "Warmeabgabe ueber den Umfang eines angelblasenen geheizten Zylinders," Forsch. Gebiete Ingenieurw. **12**, 65–73 (1933); transl. NACA TM 1050 (1943).